5th International Conference on Biaxial/Multiaxial Fatigue and Fracture Cracow'97, Poland

Paul A. BARTOLOTTA*, Peter KANTZOS** and David L. KRAUSE*

In-plane Biaxial Yield Surface Study of Cast Titanium Aluminide (TiAl)

* NASA Lewis Research Center, Cleveland, Ohio, USA
**Ohio Aerospace Institute, Cleveland, Ohio, USA

Keywords: titanium aluminide, biaxial yield surface.

Abstract: *Two cast gamma Titanium Aluminides (TiAl) were investigated at 25°C under in-plane biaxial loading conditions using cruciform specimen. Yield surfaces at an equivalent inelastic strain level of 150 microstrain (με) were generated for each TiAl. The yield surface for one of the TiAl materials exhibited a non-homogeneous behavior. Subsequent tensile tests conducted on uniaxial specimens taken from the gripping section of the cruciform specimen showed similar behavior. A microstructural study using microscopy and X-ray diffraction showed little evidence of texturing or preferential orientation of the TiAl microstructure. This paper will present the results of this study and discuss the importance of these findings.*

Introduction

Cast gamma TiAl has been identified as an alternative to conventional superalloys for advanced aeropropulsion components where high stiffness and low weight at high temperatures are required. These components are geometrically complex and are comprised of relatively thin (1.0-2.0 mm) structural elements. Typical TiAl microstructure has grain sizes ranging from 0.1 to 10.0 mm. The combination of thin structural members and large grains can provide a potential for non-homogeneous type of material behavior (i.e. anisotropy, etc). In an attempt to investigate this potential, a series of yield surface tests were conducted at room temperature on two cast gamma TiAl materials (Ti-48Al-2Cr-2Nb and XD).The tests were conducted under in-plane biaxial loading conditions at room temperature. The cruciform specimen used in these tests had a test section that is 100 mm X 100 mm in area and 2 mm thick. For both materials, an equivalent inelastic strain limit of 150 microstrain was used to define the yield surface. This small strain limit was measured using several strain gages mounted in the test section. A final equiaxed biaxial tensile test was performed for each

specimen after establishing the yield surface.
This paper will discuss the results of this study along with the observed differences between the two TiAl materials and a discussion on aspect ratios with respect to grain size and component thickness. A brief description of the unique capabilities of the new biaxial test system that was used to generate the yield surface data will also be presented.

Superalloys versus TiAl

A general comparison between cast gamma TiAl alloys and cast Ni-base superalloys material properties at room temperature is shown in table 1. From table 1, gamma does not appear to have an advantage over conventional superalloys. However, gamma does have a distinct advantage when comparing density, CTE, and thermal conductivity. All of these properties have an importance in the design of advanced aeropropulsion components. Density is important to achieve light weight components. Gamma's lower CTE can minimize thermal fatigue problems, and its higher thermal conductivity can increase its use temperature by means of ancillary cooling.

Table 1. Material Properties of Cast TiAl Alloys and Cast Superalloys at 25 °C

Property	Cast Gamma TiAl Alloys	Cast Ni-base Superalloys
Density (g/cm^3)	3.9	8.3
Yield Strength (MPa)	275-380	850
Ultimate Tensile Strength (MPa)	360-500	1000
Ductility (%)	1-3	3-5
Modulus of Elasticity (GPa)	160-175	206
Poisson's Ratio	0.27	0.29
CTE (10^{-6}/°C)	10.8	14.8
Thermal Conductivity (W/m•K)	22	11

If strength, ductility and stiffness properties are normalized with respect to their respective densities, then gamma starts to have a distinct advantage over conventional superalloys (table 2). Specific yield strength, specific ductility, and specific ultimate tensile strength of gamma alloys are similar to those of superalloys. Gamma TiAl alloys have specific modulii that are over 50% higher than superalloys. This makes TiAl more attractive for deflection limited components.

Table 2. Specific properties of TiAl alloys and superalloys normalized with respect to density

Specific Property	Cast Gamma TiAl Alloys	Cast Ni Base Superalloys
Yield Strength ($MPa/g\bullet cm^{-3}$)	70-100	102
Ultimate Tensile Strength ($MPa/g\bullet cm^{-3}$)	90-130	120
Ductility ($\%/g\bullet cm^{-3}$)	0.25-0.75	0.4-0.6
Modulus of Elasticity ($GPa/g\bullet cm^{-3}$)	41-45	25

Material Details and Tensile Properties of XD and 48-2-2

It has been shown that variability in strength, ductility, and stiffness of TiAl is associated with variations in Al content[1] which can be related, among other factors, to the TiAl microstructure. There are three basic microstructures that can be produced in TiAl depending on the Al content and material processing: equiaxed, duplex and lamellar. TiAl that is composed of either all equiaxed γ grains (fully transformed) or all lamellar colonies (γ plus α_2 phase [DO_{19} structure]) has material properties on opposite ends of the spectrum. The equiaxed structure provides for higher room temperature ductility, while the lamellar gives better fracture toughness and creep properties. The duplex structure optimizes the properties from both the lamellar and equiaxed microstructure. Composed of lamellar colonies that form interspersed about equiaxed γ grains, this duplex microstructure leads to higher strength and ductility, but lower fracture toughness. It also has been shown that Al content can influence the amount of lamellar colonies that form about equiaxed γ grains[1].

There are presently two types of TiAl that are widely being used in investment casting of aeropropulsion components: Ti-48Al-2Nb-2Cr (atomic %) and Ti-45Al-2Mn-2Nb (atomic %) + 0.8 TiB_2 (volume %), respectively named 48-2-2 and XD. The addition of TiB_2 in the XD inoculates the gamma alloy which results in refined grain sizes ranging from 100-150 μm^2. In contrast, the 48-2-2 cast material has grains several orders of magnitude larger than the XD. As seen in table 3, the refined grain size of the XD gives it a higher strength than the 48-2-2. However, with the increased strength, XD has a lower ductility and fracture toughness.

Table 3. Tensile Properties of 48-2-2 and XD at 25 °C

Property	48-2-2	XD
Yield Strength (MPa)	275-380	400-600
Ultimate Tensile Strength (MPa)	360-500	485-720
Ductility (%)	1-3	0.5-1.5
Modulus of Elasticity (GPa)	160-175	160-175
Fracture Toughness (MPa$\sqrt{m}$)	220-330	165

The general microstructure of the 48-2-2 and XD TiAl used in this study is shown in figure 1. Both alloys have a duplex microstructure which consists of g grains and a_2+g lamellar structure. XD in general has a finer microstructure and grain size and consists primarily of lamellar grains. The 48-2-2 alloy has a somewhat larger grain structure and the amount of lamellar structure varies significantly within the casting. In general, the 48-2-2 used in this study shows more variation in grain structure.

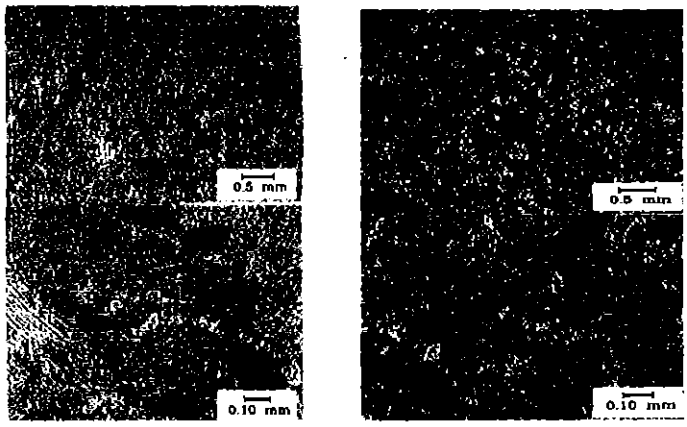

(a) (b)

Fig. 1 Microstructure of a) 48-2-2 and b) XD cast gamma TiAl.

Specimen Design and Fabrication Details

Each specimen was fabricated from a specimen blank as illustrated in figure 2a. These blanks were cast to near net shape. As shown in figure 2, the test section region of the specimen blank was cast 4 mm thicker than the final specimen thickness. Casting this oversized thickness and subsequent machining to 2 mm thickness was an attempt to eliminate the influence of surface defects (i.e., shrink and porosity) on the test results. Gating for the specimen blanks was located within one of the gripping section of the cruciform blank. To eliminate internal shrink and porosity, each specimen blank was HIPed and heat treated using the alloys' respective processes. The specimen blanks were then X-rayed to identify any internal casting defects.

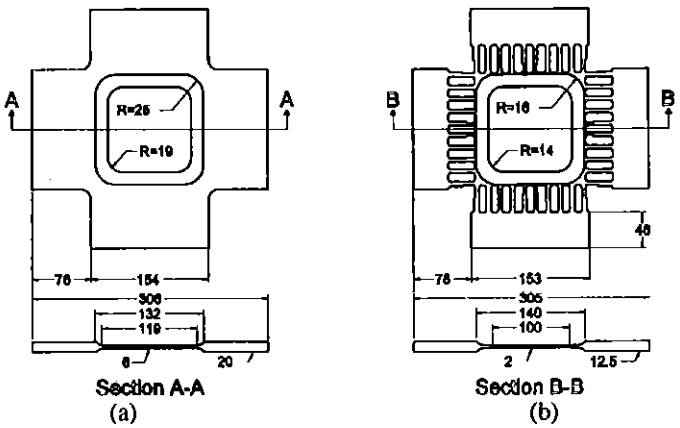

Fig. 2 General dimensions of a) near-net shape specimen blank and b) test specimen.

The biaxial test specimen used in this study was a modified version of a specimen proposed by Brown and Miller[3] for crack growth studies of monolithic alloys. Basic characteristics of this design are: its reduced section test area which provides a near constant biaxial stress state over a large range of crack lengths; slotted legs to minimize "cross-talk" between the two axes; and a single central slot to provide a high stress riser for a crack initiation site. To provide a uniform biaxial stress state for composite materials and eliminate the need for a central slot, Brown and Miller's specimen design was modified to the configuration as shown in figure 2b. The modified design incorporated a double reduced test region, tapered slots, and no central slot. This design was optimized using a FEA parametric study. The final FEA of the specimen indicated that the stress distribution within the center test region was within ±5.0 % of the nominal stress.

Test Equipment and Experimental Procedure

The in-plane biaxial test system[4] used in this study consisted of: i) four 490 kN hydraulic actuators, two in each direction, that applied the mechanical loads to the plate specimen, ii) four water cooled hydraulic wedge grips that were aligned to a bending strain in each axis of less than 10% bending at 100 mm/mm, and iii) a state-of-the-art digital controller. The controller monitored and provided signal conditioning for each load and actuator position channel.

The digital controller allowed each actuator to be controlled independently or in centroid control. Centroid control mode uses a master-slave relationship between two opposing actuators in the same axis to maintain the center of the specimen within ± 25 μm from the center of the load frame. Ensuring that the centers of the specimen and load frame coincide aids in preventing off-axis loading which would damage the opposing actuators. In addition, centroid control assists in maintaining a uniform stress state in the specimen test area.

Strains for each specimen were measured using 90° rosettes located throughout the test section of the specimen (fig . 3). During the tests, the test control and data acquisition were performed by a computer using object-oriented control software. The software uses a series of virtual instruments that were linked together to create a custom test control program. As the specimens were loaded biaxially, the control program monitored both X-axis and Y-axis strains until a predetermined equivalent inelastic strain level was achieved. At that point, the control software quickly unloaded the specimen to a zero load condition.

Fig.3 Test set-up showing biaxial specimen with strain gages in the load frame.

Yield surface probe/biaxial tensile tests were conducted under in-plane biaxial loading conditions at room temperature. For both materials, an equivalent inelastic strain limit of 150 με was used to define the yield surface. The level of 150 με was chosen to minimize any hardening (or softening) effect from the loading. Therefore, the yield surface was defined using one specimen for each TiAl material.

In this study, all yield surface probes were conducted in load control using a loading rate in both axis of 35 Pa/sec. Changes in biaxial stress states were achieved by changing the ratios of loads along the two axes. For each TiAl material, after the yield surface was defined an equiaxed biaxial tensile test was conducted and the measured equivalent ultimate tensile strength was compared to predicted values based on uniaxial tensile tests.

After observing the preferential yield surface results of the 48-2-2 material, it was decided to perform subsequent uniaxial tensile tests on specimens fabricated from the "undisturbed" gripping section of the biaxial specimen. These specimens were machined from blanks taken from both the X-axis and Y-axis gripping sections of the 48-2-2 specimen. Three specimen blanks at each section were fabricated by wire EDM through the thickness of the grip section. Each blank was cut 2 mm oversized (4 mm thick) and was carefully surface ground to a final nominal thickness of 2 mm. A total of 6 dog-boned specimens were machined from each section. The dog-bone specimens had 28 mm long test section with polished edges. The uniaxial tensile tests were conducted under strain control at a constant strain rate of 10^{-4}/sec.

Experimental Results

Yield surface probe results for both 48-2-2 and XD are shown in figure 4 along with a reference 310 MPa yield surface. As illustrated in figure 4, the XD material (square symbols) exhibited a 150 με yield surface typical to a polycrystalline material. Contrary, the 48-2-2 yield surface (circle symbols) indicated a preferential yield in the "Y" loading axis, typical for a material that has a textured microstructure. Note for the 48-2-2, the X-axis had a higher yield stress than the Y-axis stress. The 48-2-2 yield surface (dashed line), as defined by the probes, was oblong and leaning over compared to the XD surface which was symmetrical and oriented with a 45° incline. Also note that even though the XD has a larger yield strength than 48-2-2, the magnitudes of the resultant yield surfaces for 150 με inelastic strain were very close.

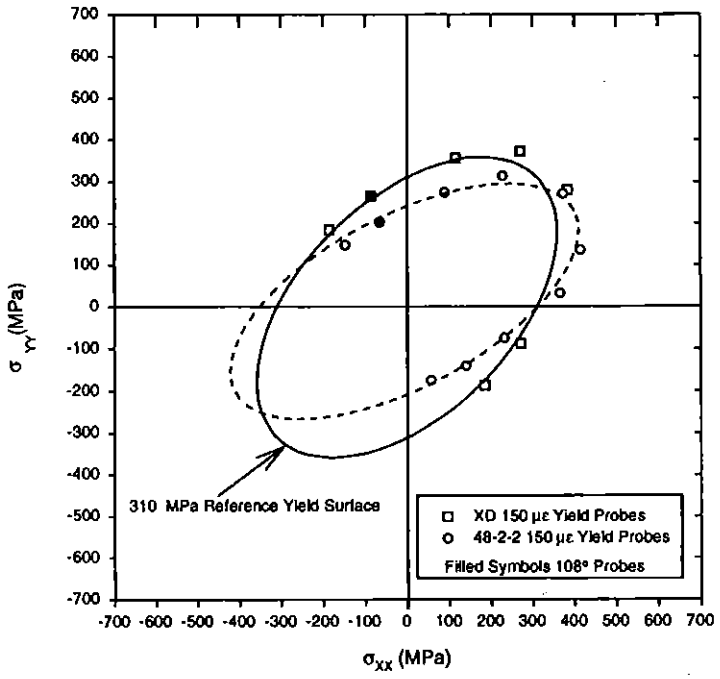

Fig.4 150 με yield surfaces for XD and 48-2-2 at 25 °C.

To illustrate the uniform stress/strain distribution within the test section of the biaxial specimen, equivalent stress - strain response for several strain gages are shown in figure 5. The equivalent stress - strain responses presented in figure 5 are from the 108° yield surface probes which are denoted in figure 4 by filled symbols. The 48-2-2 specimen exhibited a slightly larger variation of strains in its test section (fig 5b) with the largest difference being 170 με. This trend was typical for all of the 48-2-2 probes. For the XD specimen, the strain distribution was especially uniform with the largest difference in strain being 105 με (fig 5a). Once again, this was typical for all of the XD probes.

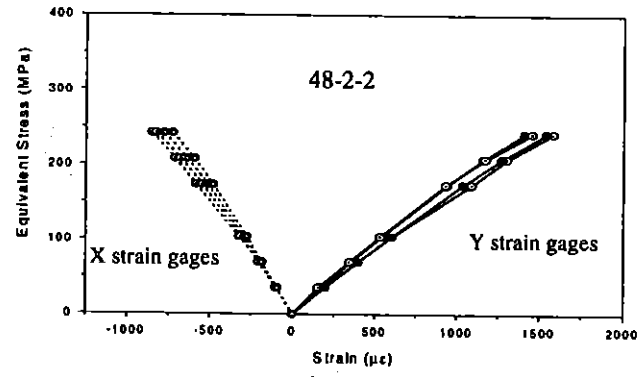

(a)

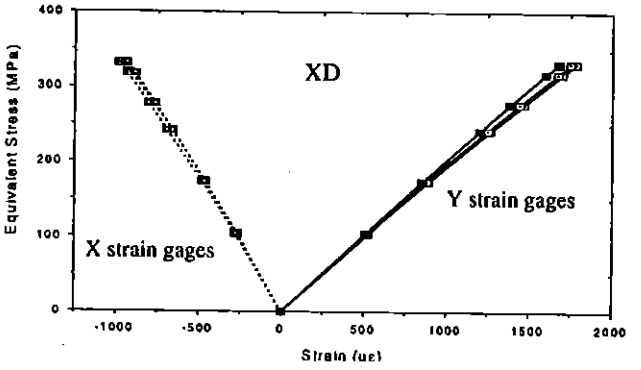

(b)

Fig.5 Strain gage response for 108° yield probe for a) 48-2-2 and b) XD at 25 °C.

After the yield surface probes were completed for both specimens, an equiaxed tensile test was performed. The equivalent failure stresses measured for both materials were 448 MPa for XD and 414 MPa for 48-2-2. It is debatable on whether the observed anisotropy of the 48-2-2 influenced the final biaxial tensile test results. Figure 6 shows a typical failure mode for these tests. The fracture surfaces for both materials show similar crack trajectories which were both intergranular and transgranular.

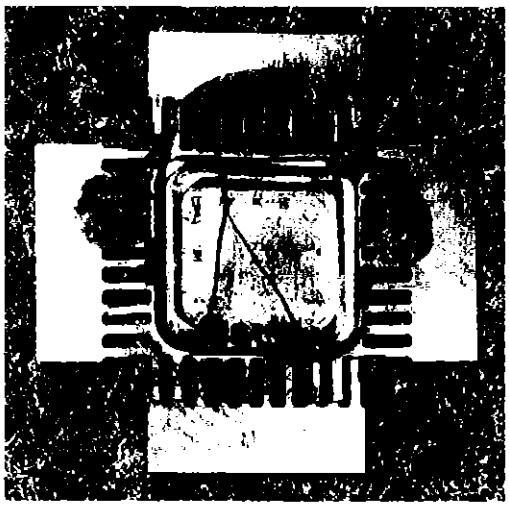

Fig.6 Failed XD specimen after equiaxed tensile test conducted at 25 °C.

A series of uniaxial tensile tests were conducted on specimens fabricated from the gripping sections of the 48-2-2 specimen. These tests were conducted in an attempt to quantify the observed non-homogeneous biaxial yield behavior of the 48-2-2. The tensile mean properties for each direction (X and Y) are presented in table 4. Note that the X direction specimens had higher yield strength and elastic modulus and lower ductility than those specimens that represented the Y direction. This difference is what was expected if there was a preferential material direction in a wrought material. However, these results are within the within the normal statistical scatter of a cast 48-2-2 tensile properties (table 3).

Table 4. Average uniaxial tensile properties of sectioned 48-2-2 biaxial specimens at 25 °C

Property	X direction specimens	Y direction specimens
Yield Strength (MPa)	383.6	375.6
Ultimate Tensile Strength (MPa)	422.9	426.0
Ductility (%)	0.68	0.80
Modulus of Elasticity (GPa)	196.9	187.2

Microstructural Study Results

A macro-etching technique has shown flow patterns within the grain structure of the 48-2-2 material. The same etching technique showed no flow patterns for the finer grained XD material. Further microstructural examination of the 48-2-2 specimen was conducted to identify the cause of the observed anisotropic behavior. X-ray diffraction was conducted on several samples from the test section of the 48-2-2. Results from the X-ray diffraction were inconclusive for texturing. One sample indicated some type of texture, however, it could

have been a reading off one of the significantly large grains of the 48-2-2. Other samples showed little or no indication of texture.

Difference in the grain structure between these alloys in figure 1. It is even more evident within the thin gage section, figure 7. In some cases, 48-2-2, has only several (1-3) grains through the thickness compared to >10 grains for alloy XD. Some of the larger lamellar grains in 48-2-2 may consist of smaller sub-grains with low angle grain boundaries. This could account for some of the confusing readings from the X-ray diffraction.

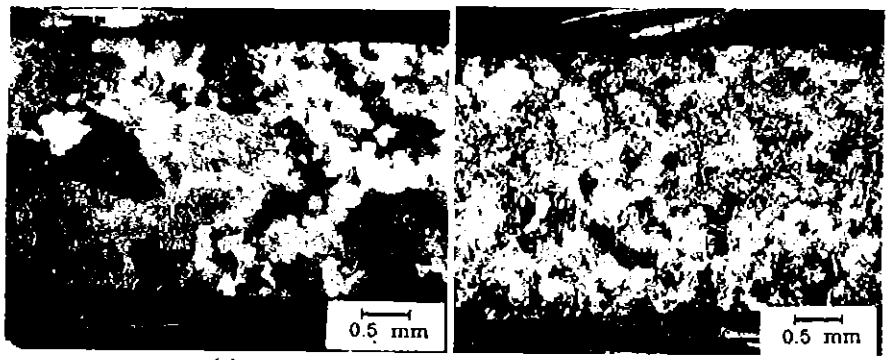

Fig. 7 Microstructure of a) 48-2-2 and b) XD test sections.

The lamellar grains in 48-2-2 also show some preferred orientation, as shown in figure 8, the lamella tend to be parallel to the cast surfaces. These observations may also contribute to the observed anisotropy in 48-2-2. The tensile specimens which were taken from the grip ends did not show much of an effect from preferential lamellar orientation. However, it should be noted that these specimens were also very close to the gates for both X and Y gripping areas.

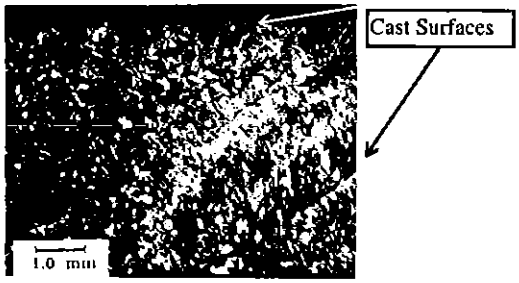

Fig. 8 Microstructure of 48-2-2 specimen near the surface of the gripping area .

This grain orientation can be contributed to the solidification process of the 48-2-2 casting. As the casting cools, the outer layers of material solidifies first. Since 48-2-2 grains are relatively large this forms a layer of grains. As the solidification process continues through the thickness of the casting, more of this structured grain layers are formed. In figure 8, the layers of grains are quite evident (Note: the dashed white line to identify the orientation of

the solidification process).

Discussion

Cast gamma is currently being used and considered for aeropropulsion components as a substitute for Ni-base superalloys because of its superior specific properties. Like all advanced materials, cast TiAl has its advantages and disadvantages. In general, designers should take account cast gamma's low ductility, toughness, and fatigue resistance when considering it for an application. In designing component attachment points and interfaces, careful consideration should be placed on the differences in thermal expansion characteristics between gamma and other materials. For instance, due to its relatively low thermal expansion trait, a TiAl-to-superalloy joint could produce a significantly high thermal stress in the gamma component causing a premature failure. As suggested by the results from this study, designers should also consider the potential for cast 48-2-2 to behave in a anisotropic non-homogeneous manner.

From figure 4, it was shown that the XD material exhibited a room temperature yield surface of a isotropic homogeneous material. Likewise, its microstructure showed the same characteristics. The yield surface of the 48-2-2 material was oblong and had a preferential direction. This behavior is similar to a material that has a texture. As shown in figure 1 and 7, the microstructure of 48-2-2 vastly differs from the XD material.

Figure 5 further substantiates the argument that the differing microstructure could have an influence on the anisotropic property of the 48-2-2. Ignoring the obvious differences of stiffness and strength, the strain response within the XD specimen test section (fig 5b) exhibits little or no variation throughout the yield probe. This response is indicative to a fine grained homogeneous material. In comparison, the 48-2-2 strain responses within the test section (fig 5a) varies significantly throughout the probe. The variation is as great as 20% of the average measured strain. It can be argued that this variation in the strain response is attributed to the larger grain/colony size that the cast 48-2-2 has with respect to the thickness of the specimen test section. Due to the cast 48-2-2 microstructure, the strain gages in the test section were not sensing the deformation of a large volume of grains/colonies like in the XD specimen. Instead the gages were sensing the deformation of 1-3 grains/colonies, each with different preferential orientations and behaviors. For the XD specimen, due to its refined microstructure, the strain gages actually were averaging strains over many more slip systems than for the 48-2-2. The grains per unit thickness for the XD specimen was much greater than that of the 48-2-2. This is the main reason why the XD material behaved in a uniformed isotropic manner and the 48-2-2 exhibited anisotropic behavior.

The results of the post probe uniaxial tensile tests of the 48-2-2 showed typical scatter (table 4) in the properties and, therefore, no definitive evidence about preferential orientation was obtained. In hindsight, these tensile specimens should have been manufactured from the test section of the biaxial specimen. The gripping area is too close to the gating and is cast thicker than the test area, therefore, this material is not representative of the test area.

Being a cast material, cast 48-2-2 is subjected to the same casting issues (i.e., gating, shrink, solidification rates, porosity, etc.) as other cast materials. This study showed that the aspect ratio between component thickness and grain/colony size can influence its mechanical properties. Another similar issue has been observed for cast 48-2-2 and is illustrated in figure 9[5]. As seen in figure 9. the microstructure of one end of a cast 48-2-2 slab is significantly different from the other. At one end, a 77 volume fraction of the γ-α_2 lamellar colonies was found and the opposite end a 48 volume fraction.

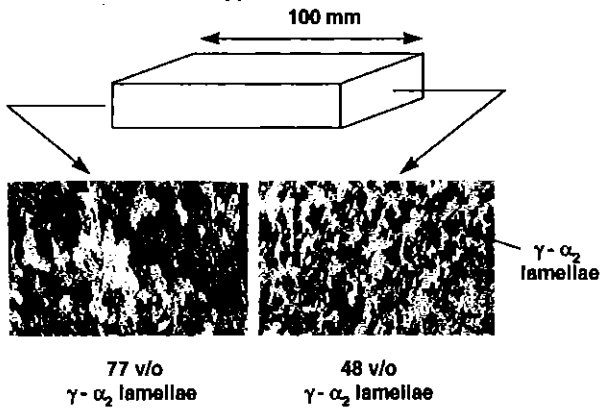

Fig. 9 Differences in microstructure within a 48-2-2 cast slab[5].

At first glance, the ramifications from this observation can be problematic in the use of 48-2-2 in two dimensional components such as flaps and turbine blades. However, through the use of intelligent material processing, this difference in microstructure can be used to an advantage. This is especially true for turbine blades. An optimized turbine blade design can significantly benefit from a material that has a high strength / fatigue resistance at its root and, at the same time, a high creep resistance in its body. By learning how to control the microstructure in a 48-2-2 via intelligent material processing a better turbine blade can be developed. This represents an area for further 48-2-2 processing research. Present cast 48-2-2 applications have been limited to axisymmetrical components like diffusers. ducts, and cases (figure 10).

In these axisymmetrical applications, differences in cast microstructure can produce within the casting areas of low creep resistance, low strength, or low fatigue resistance. However, due to the way these components are gated, poured and cooled, these areas are typically confined to an axisymmetrical location in the part. Remedies for this phenomena are simple and straightforward, requiring slight changes in gating and/or cooling methods, or a change in component design.

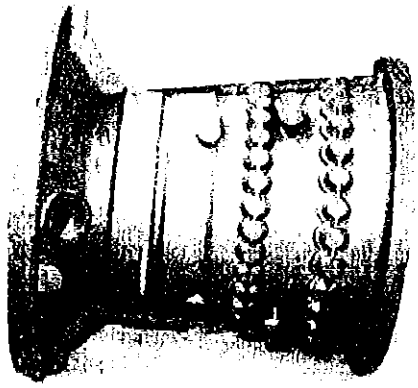

Fig. 10 Cast 48-2-2 compressor case.

For 2-D components, like a rib-stiffen flap, it is a little more complicated. Due to the 2-D gating, cooling rates, and the 2-D geometry of the cast component, differences in microstructure can be located in different areas throughout component that are not necessarily symmetrical with respect to each other (fig 11). Here lies an area for further development in smart material processing of cast 2-D 48-2-2 components. Through smart processing of these cast 48-2-2 components, a designer can capitalize on the advantages of being able to control the microstructure to provide required material properties where they will maximize the component's design.

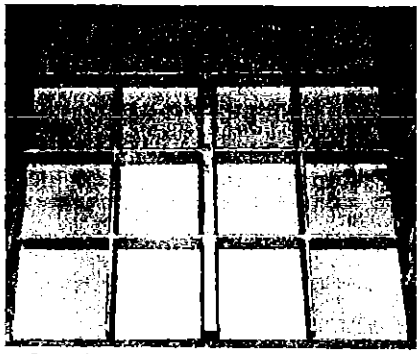

Fig. 11 Cast, rib stiffen face sheet fabricated from 48-2-2

Summary

A study investigating the room temperature yield behavior of two cast TiAl materials, namely XD and 48-2-2, has been completed. Yield probes were used to define the 150 με yield surface for each material. The yield surface for the XD material exhibited the shape and orientation of an homogeneous isotropic material while the 48-2-2 yield surface indicated preferential yielding had occurred. Subsequent uniaxial tensile tests of specimens

fabricated from the 48-2-2 show little to no indications of a preferential yield direction. A microstructural study was conducted to determine the cause of the anisotropic behavior of the 48-2-2. Results from X-ray diffraction were inconclusive due to the 48-2-2 large grains/colonies. There was some indications of a structured orientation of the 48-2-2 grains due to the solidification process. The observed differences in the yield surfaces between 48-2-2 and XD can be contributed to 48-2-2's low grains to unit thickness ratio within the test section of the biaxial specimen. For XD, this ratio is relatively higher than the 48-2-2. Designers should be aware of the relationship of grain/colony size and component thickness when considering 48-2-2 for a 2-D component. Further studies on the processing of cast 48-2-2 should be conducted in order to tailor this material to capitalize on the variable microstructures that can emerge in a 2-D component casting.

References

1 Nishiyama, Y., Miyashita, T., Isobe, S., and Noda, T., "Proceedings of 1989 Symposium on High Temperature Aluminides and Intermetallics", 1989, pp557-573.

2 Larsen, D.E., Wheeler, D.A., and London, B., "Processing and Manufacture of Gamma and XD™ Gamma Titanium Aluminide Components by Investment Casting", Proceedings of Processing and Fabrication of Advanced Materials III, TMS,1994,pp631-641.

3 Brown, M.W. and Miller, K.J.:"Mode I Fatigue Crack Growth Under Biaxial Stress at Room and Elevated Temperature," Multiaxial Fatigue, ASTM STP 853, K.J.Miller and M.W.Brown, Eds.,ASTM, Philadelphia, 1985, pp.135-152.

4 Bartolotta, P.A., Ellis,J.R., and Aziz, A., "A Structural Test Facility for In-Plane Biaxial Testing of Advanced Materials," Multiaxial Fatigue and Deformation Testing Techniques, ASTM STP 1280, S. Kalluri and P. J. Bonacuse, Eds., ASTM, 1997, pp. 25-42.

5 Unpublished data from Drs. Rebecca MacKay and Ivan Locci, NASA Lewis Research Center, 1996.

Acknowledgments

The authors wish to acknowledge Mr. Steve Smith for his efforts in the laboratory.